

The fidelity approach to the Hubbard model

L. Campos Venuti,¹ M. Cozzini,^{1,2} P. Buonsante,^{3,2} F. Massel,² N. Bray-Ali,⁴ and P. Zanardi^{4,1}

¹*ISI Foundation for Scientific Interchange, Villa Gualino, Viale Settimio Severo 65, I-10133 Torino, Italy*

²*Dipartimento di Fisica, Politecnico di Torino, Corso Duca degli Abruzzi 24, I-10129 Torino, Italy*

³*CNISM, Unità di Ricerca Torino Politecnico, Corso Duca degli Abruzzi 24, I-10129 Torino, Italy*

⁴*Department of Physics and Astronomy, University of Southern California Los Angeles, California 90089-0484, USA*

(Dated: February 6, 2020)

We use the fidelity approach to quantum critical points to study the zero temperature phase diagram of the one-dimensional Hubbard model. Using a variety of analytical and numerical techniques, we show that the metal-insulator phase transitions featured by the system can be insightfully analyzed in terms of the fidelity metric tensor. In particular at the infinite order Mott transition the fidelity metric shows divergences depending on the path of approach to the critical point.

PACS numbers: 64.60.-i, 03.65.Ud, 05.70.Jk, 05.45.Mt.

I. INTRODUCTION

Recently a novel characterization of phase transitions has been advocated [1]. This is the so called fidelity approach to critical phenomena [2, 3, 4, 5, 6, 7, 8, 9, 10, 11, 12, 13, 14, 15, 16] that relies solely on the state of the system and does not require the knowledge of the model Hamiltonian and its symmetry breaking mechanism. Two states of the system at nearby points in parameter space are compared by computing their overlap (the fidelity). Since quantum phase transitions are major changes in the structure of the ground state, it is natural to expect that, when one crosses a transition point the fidelity will drop abruptly. To make the analysis more quantitative one considers the second derivative of the fidelity with respect to the displacement in parameter space. Remarkably this second derivative, more in general the Hessian matrix, defines a metric tensor (the fidelity metric hereafter) in the space of pure states [16]. A super-extensive scaling of the fidelity metric corresponds to the intuitive idea of a fidelity drop. Indeed, it was shown in [17] that, at regular points the fidelity metric scales extensively with the system size, and a super-extensive behavior implies criticality. However the converse is not true in general; in order to observe a divergence in the fidelity metric a sufficiently relevant perturbation (in the renormalization group sense) is needed [17]. Loosely speaking the more relevant the operator the stronger the divergence of the fidelity metric. The Berezinskii-Kosterlitz-Thouless (BKT) transition is peculiar in this respect as it is driven by a marginally relevant perturbation, i.e. with the smallest possible scaling dimension capable of driving a transition. This gives rise to an infinite order transition and as such the BKT does not rigorously fit in the simple scaling argument given in [17]. Surprisingly, contrary to the naïve expectation, Yang has shown [15] that in the particular instance of BKT transition provided by the XXZ model, the fidelity metric diverges algebraically as a function of the anisotropy. This is an appealing feature since the gap opens up very slowly at a BKT transition and so

observing a singularity is generally a difficult task [36].

In this article we study a paradigmatic example of correlated electrons in one dimension, the celebrated Hubbard model, from the point of view of the fidelity approach. This will allow us to investigate both a BKT transition as well as a more conventional band-insulator transition. In the 1D Hubbard model the BKT transition [37] occurs exactly at half filling as soon as the on site interaction U is switched on, inducing a gap in the charge excitation spectrum. Away from half filling instead all modes are gapless for any U and the system is a Luttinger liquid. Since at half filling, the only gapless point is at $U = 0$, the kind of BKT transition offered by the Hubbard model is different from that featured by the XXZ model. In that case one continuously arrives at the transition point from a gapless phase by tuning the anisotropy parameter. This difference, in turn, makes more difficult the analysis of the fidelity metric in the Hubbard model. By resorting to both bosonization and Bethe-Ansatz techniques, we will show that some sort of divergences in the fidelity metric are present.

II. PRELIMINARIES

The one dimensional Hubbard model is given by

$$H = -t \sum_{i,\sigma} \left(c_{i,\sigma}^\dagger c_{i+1,\sigma} + \text{h.c.} \right) + U \sum_i n_{i,\uparrow} n_{i,\downarrow} - \mu \sum_i n_i, \quad (1)$$

where $n_{i,\sigma} = c_{i,\sigma}^\dagger c_{i,\sigma}$, $n_i = n_{i,\uparrow} + n_{i,\downarrow}$ and we will be concerned with the repulsive / free gas case when $U \geq 0$. Due to the symmetries of the model [18] it is sufficient to limit the analysis to filling smaller or equal to one half i.e. $n \equiv \langle n_i \rangle \leq 1$. It is well known [19, 20] that for $n < 1$ the model is in the Luttinger liquid universality class for any value of the interaction U . Spin and charge degrees of freedom separate and their respective excitations travel at distinct velocities v_s and v_c . Both charge and spin modes are therefore gapless. Exactly at half filling ($n = 1$) the system becomes an insulator and develops a charge gap $\Delta E_c = \mu_+ - \mu_- = E(N+1) - 2E(N) + E(N-1)$,

where $E(N)$ is the ground state energy with N particles. The gap opens up exponentially slow from $U = 0$, and the point $U = 0, n = 1$ is a transition of BKT type [21]. The length scale $\xi = 2v_c/\Delta E_c$ describes the size of soliton-antisoliton pairs, in the insulator. As we approach the critical point at $U = 0, n = 1$, these pairs unbind and proliferate, allowing the system to conduct.

In the fidelity approach one is interested in the overlap between ground states at neighboring points of the coupling constants (say a vector λ): $F(\lambda) = |\langle \psi(\lambda) | \psi(\lambda + d\lambda) \rangle|$. Remarkably, the second order term in the expansion of the fidelity defines a metric in the space of (pure) states:

$$F(\lambda) = 1 - \frac{1}{2} G_{\mu,\nu} d\lambda^\mu d\lambda^\nu + O(d\lambda^3),$$

where

$$G_{\mu,\nu} = \text{Re} [\langle \partial_\mu \psi_0 | \partial_\nu \psi_0 \rangle - \langle \partial_\mu \psi_0 | \psi_0 \rangle \langle \psi_0 | \partial_\nu \psi_0 \rangle],$$

and $\psi_0 = \psi(\lambda)$ and $\partial_\mu = \partial/\partial\lambda^\mu$. Actually, at regular points λ of the phase diagram, $G_{\mu,\nu}$ is an extensive quantity [17] so that it is useful to define the related intensive metric tensor $g_{\mu,\nu} \equiv G_{\mu,\nu}/L$. With reference to Hamiltonian (1) it is natural to investigate the behavior of the fidelity under variations of the interaction parameter U . The possibility of analyzing variations of the chemical potential, though appealing does not fit in the fidelity approach as the ground states at different μ belong to different super-selection sectors. Hence now on we will solely be interested in $g_{U,U}$ and we will simply write g in place of $g_{U,U}$. In Ref. [16] it was shown that it can be written in the following form

$$g = \frac{1}{L} \sum_{n>0} \frac{|V_{n,0}|^2}{(E_n - E_0)^2}, \quad V = \sum_i n_{i,\uparrow} n_{i,\downarrow} \quad (2)$$

where $E_n, |n\rangle$ are the eigen-energies and corresponding eigenstates of the Hamiltonian (1) (with repulsion U and filling n), $|0\rangle$ corresponds then to the ground state and $V_{i,j} = \langle i | V | j \rangle$. In passing, we would like to notice that despite the apparent similarity between Eq. (2) and the second derivative of the energy $E''(\lambda)$ (a similarity stressed in Ref. [22]), it is possible to show – using the Rayleigh-Schrödinger series – that the metric tensor is in fact related to the third (and first) energy derivative, via

$$G = \frac{1}{V_{0,0}} \sum_{i,j>0} \frac{V_{0,i} V_{i,j} V_{j,0}}{(E_i - E_0)(E_j - E_0)} - \frac{E'''}{E'}.$$

Moreover, in cases where $E'''(\lambda)$ is bounded in the thermodynamic limit, one obtains the interesting kind of factorization relation $\langle 0 | V | 0 \rangle \langle 0 | V \mathcal{G}(E_0)^2 V | 0 \rangle = \langle 0 | V \mathcal{G}(E_0) V \mathcal{G}(E_0) V | 0 \rangle$ valid in the thermodynamic limit, where \mathcal{G} is the resolvent $\mathcal{G}(E) = (\mathbb{1} - |0\rangle\langle 0|)(H - E)^{-1}(\mathbb{1} - |0\rangle\langle 0|)$.

In the rest of the paper we will be concerned with the analysis of the metric tensor with special care to the BKT

transition point. The phase diagram of the Hubbard model is depicted in Fig. 1. The model has been solved by Bethe Ansatz in Ref. [23]. We will tackle the problem using a variety of techniques. On the free-gas $U = 0$ line, an explicit calculation is possible at all fillings. Around the region $U = 0$ and filling away from $n = 0$ and $n = 1$ bosonization results apply. Instead, close to the points $U = 0$ and $n = 0, 1$ we will cross results from bosonization with Bethe-ansatz in order to extend bosonization results up to the transition points. Finally we will report numerical results on the massive $n = 1$ line.

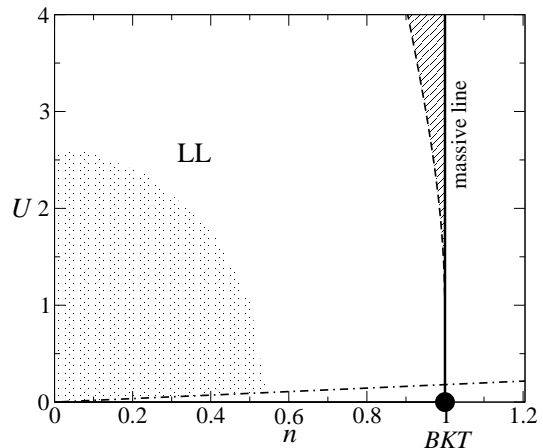


Figure 1: Phase diagram of the repulsive Hubbard model. The region $0 < n < 1$ is in the Luttinger liquid (LL) universality class. The dotted and hatched areas correspond to the conditions $na(U) < 1$ and $\delta a(U) < 1$ respectively, see Sec. V. Deep in these regions ($na(U) \ll 1$ and $\delta a(U) \ll 1$) an expansion around $n = 0, n = 1$ is possible.

III. EXACT ANALYSIS AT $U = 0$

At $U = 0$ the complete set of eigenfunctions of Hamiltonian (1) is given by a filled Fermi sea and particle-hole excitations above it. It is then possible to apply directly Eq. (2).

A. Half filling

We first treat the half filled case $n = 1$, where the Fermi momentum lies at $k_F = \pi/2$. Writing the interaction in Fourier space as $V = L^{-1} \sum_{k,k',q} c_{k'-q,\downarrow}^\dagger c_{k+q,\uparrow}^\dagger c_{k,\uparrow} c_{k',\downarrow}$, and going to the thermodynamic limit, Eq. (2) becomes

$$g = \frac{1}{(2\pi)^3} \int_{[-\pi,\pi]^3} \frac{n_k (1 - n_{k+q}) n_{k'} (1 - n_{k'-q})}{(\epsilon_{k+q} - \epsilon_k + \epsilon_{k'-q} - \epsilon_{k'})^2} dk dk' dq, \quad (3)$$

where $\epsilon_k = -2t \cos(k)$ is the $U = 0$ single particle dispersion and $n_k = \vartheta(-\epsilon_k)$ ($= n_{k,\uparrow} = n_{k,\downarrow}$ in absence of magnetic field) are the fermionic, zero-temperature, filling factors. Using $\epsilon(k, q) \equiv \epsilon_{k+q} - \epsilon_k = 4 \sin(q/2) \sin(k + q/2)$ and substituting $k' \rightarrow -k'$ we obtain

$$g = \frac{1}{(2\pi)^3} \int_0^\pi dq \frac{1}{8 \sin(q/2)^2} \int_{-\pi}^\pi dk \int_{-\pi}^\pi dk' \times \frac{n(k, q) n(k', q)}{[\sin(k + q/2) + \sin(k' + q/2)]^2}.$$

Changing variables to $p = k + q/2$, $p' = k' + q/2$ and making a shift of $\pi/2$ we obtain finally

$$g = \frac{1}{(2\pi)^3} \int_0^\pi dq \frac{J(q)}{8 \sin(q/2)^2} = \frac{1}{24\pi^2} = 0.00422 \quad (4)$$

where we defined

$$\begin{aligned} J(q) &= 4 \int_0^{q/2} dp \int_0^{q/2} dp' \frac{1}{[\cos(p) + \cos(p')]^2} \\ &= -2 + 8 \frac{\ln(\cos(q/2))}{\cos(q) - 1}, \end{aligned}$$

and correctly $J(q) = J(-q) > 0$.

A related interesting issue is that of the finite size scaling of the metric tensor g i.e. the way in which g_L at length L converges to its thermodynamic value (see also [6]). In Ref. [17] it was shown that in a gapless regime scaling analysis predicts $g_L \sim L^{-\Delta_g}$ apart from regular contributions which scale extensively (and contribute to g with a constant). Here $\Delta_g = 2\Delta_V - 2\zeta - 1$ where Δ_V is the scaling dimension of V in the renormalization group sense and ζ is the dynamical critical exponent. On the line $U = 0$ one has $\Delta_V = 2$ as V is a product of two independent free fields, while $\zeta = 1$ when $n \neq 0$ due to the linear dispersion of excitations at low momenta. This implies that at leading order $g_L \sim A + BL^{-1}$. One should however be careful that logarithmic corrections are not captured by the scaling analysis of Ref. [17] and they might be present due to the BKT transition occurring at this point. Let us try to clarify this issue. Looking at Eq. (4), as a first approximation, we might think that the finite size g_L is well approximated by the Riemann sum of $F(q) \equiv J(q) / \sin(q/2)^2$:

$$g_L \simeq \frac{S_L}{(2\pi)^3 8}, \quad S_L = \frac{2\pi}{L} \sum_{n=1}^{L/2} F\left(\frac{2\pi}{L}n\right).$$

Now $F(q)$ diverges logarithmically around π^- : $F(q) = -4 \ln(\frac{\pi-q}{2}) + O((\pi-q)^2)$, and since the Riemann sum of the logarithm converges to its integral as $(A + B \ln L)/L + O(L^{-2})$ we would conclude

$$g_L - \frac{1}{24\pi^2} = \frac{A + B \ln L}{L} + \frac{C}{L^2} + O(L^{-4}). \quad (5)$$

However, a detailed analysis of the finite size g_L reveals that a *cancellation* occurs between two logarithmic corrections so that actually $B = 0$ in Eq. (5). The exact finite size g_L is composed of two terms. One term is a triple sum which, in the thermodynamic limit, corresponds to the triple integral in Eq. (3). The other term is a double sum which originates from zero transferred momentum contribution and vanishes when $L \rightarrow \infty$. We numerically verified that both terms contain a $\ln L/L$ part when $L \rightarrow \infty$, but their contribution is equal and opposite so as to cancel out exactly from g_L . The absence of logarithmic corrections can clearly be seen in the inset of Fig. 2 where the finite size g_L is plotted against $1/L$.

B. Away from half filling

Similar considerations can be done away from half-filling. Eq. (3) still holds, simply in this case $k_F \neq \pi/2$. We assume $k_F = n\pi/2 < \pi/2$ (anyway a particle hole transformation implies $g(n) = g(2-n)$). First note that the integral over q can be recast as $2 \int_0^\pi dq$. The filling factors constrain the momenta to $|k| < k_F$ and $|k + q| > k_F$. If $q < 2k_F$ this implies $k_F - q < k < k_F$. Instead if $q > 2k_F$ the sum over k is unconstrained: $-k_F < k < k_F$. Thus we obtain

$$\begin{aligned} g &= \frac{2}{(2\pi)^3} \left\{ \int_0^{2k_F} dq \int_{k_F-q}^{k_F} dk \int_{k_F-q}^{k_F} dk' \right. \\ &\quad \left. + \int_{2k_F}^\pi dq \int_{-k_F}^{k_F} dk \int_{-k_F}^{k_F} dk' \right\} \\ &\quad \times \frac{1}{16 \sin(q/2)^2 [\sin(k + q/2) + \sin(k' + q/2)]^2}. \end{aligned}$$

Changing variables as before and defining

$$J(a, b) \equiv \int_a^b dp \int_a^b dp' \frac{1}{[\sin(p) + \sin(p')]^2},$$

we obtain

$$\begin{aligned} g &= \frac{1}{64\pi^3} \left\{ \int_0^{2k_F} dq \frac{J(k_F - q/2, k_F + q/2)}{\sin(q/2)^2} \right. \\ &\quad \left. + \int_{2k_F}^\pi dq \frac{J(-k_F + q/2, k_F + q/2)}{\sin(q/2)^2} \right\}. \end{aligned}$$

In Fig. 2 one can see a plot of $g(n, U = 0)$ as a function of the total density $n = N_{\text{tot}}/L = 2k_F/\pi$. It is possible to show that in the very dilute regime $n \rightarrow 0$, the fidelity metric g diverges in a simple algebraic way

$$g(n \rightarrow 0, U = 0) \sim \frac{1}{n}.$$

This divergence can also be simply understood by resorting to the scaling arguments reported in [17]. There

it was shown that, in the thermodynamic limit $g \sim |\mu - \mu_c|^{\Delta_g/\Delta_\mu}$ where now Δ_μ is the scaling dimension of the field μ . On the line $U = 0$ as already noticed $\Delta_V = 2$ while now $\zeta = 2$ as $n \rightarrow 0$ to account for the parabolic dispersion. The chemical potential scaling exponent is $\Delta_\mu = 2$ in the dilute Fermi gas [24]. All in all we obtain $g \sim |\mu - \mu_c|^{-1/2} \sim n^{-1}$ since $n \sim |\mu - \mu_c|^{1/2}$ which agrees with the explicit calculation.

The finite size scaling of g_L for different filling $0 < n < 1$ is the same as that observed at $n = 1$ and is dictated by Eq. (5) with $B = 0$, as can be seen in the inset of Fig. 2.

Finally note that, since $g(n, U = 0)$ is symmetric around $n = 1$, $g(n)$ has a local maximum at that point with a cusp. The origin of this discontinuity is not well understood at the moment but reveals a signature of the t.

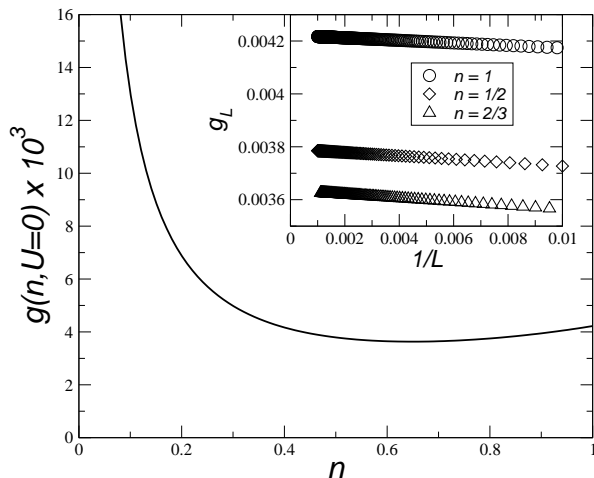


Figure 2: Fidelity metric g as a function of the total density at $U = 0$. The singularity at $n \rightarrow 0$ is of the form n^{-1} . In the inset the finite size scaling of g_L for some different fillings is shown. The approach to the thermodynamic value is given by Eq. (5) with $B = 0$. In fact fitting the data points with Eq. (5) gives values of B/A of the order of 10^{-4} and a chi-square of the same order as the one obtained with $B = 0$.

IV. BOSONIZATION APPROACH

It is well known [18, 19, 25] that for $U \geq 0$ and away from half filling ($n = 1$), the low energy, large distance behavior of the Hubbard model, up to irrelevant operators, is described by the Hamiltonian

$$H = H_s + H_c \quad (6)$$

$$H_\nu = \frac{v_\nu}{2} \int d^2x \left[K_\nu \Pi_\nu(x)^2 + \frac{1}{K_\nu} (\partial_x \Phi_\nu)^2 \right], \quad \nu = s, c.$$

Charge and spin degrees of freedom factorize and are described respectively by H_c and H_s . The Luttinger liquid

parameters $K_{c,s}$ are related to the long distance, algebraic decay of correlation functions, while $v_{c,s}$ are the speed of elementary (gapless) charge and spin excitations. From bosonization, and setting the lattice constant $a = 1$, one finds, for small U ,

$$K_c = 1 - \frac{U}{2\pi v_F} + \dots, \quad (7)$$

where the Fermi velocity is $v_F = 2t \sin(k_F)$ and $k_F = \pi n/2$. Instead the Luttinger parameter K_s is fixed to $K_s = 1$ due to spin rotation invariance. Exactly at $n = 1$ there appears another term (an Umklapp term) in the charge sector which is marginally relevant and is responsible for the opening of a mass gap. In this case the effective theory is the sine-Gordon model.

Since the fidelity of two independent theories factorizes the metric tensor g is additive and we obtain $g = g_s + g_c$. In Ref. [15] the fidelity metric of a free boson theory has been calculated to be given by

$$g_\nu = \frac{1}{8} \left(\frac{1}{K_\nu} \frac{dK_\nu}{dU} \right)^2. \quad (8)$$

In our case $g_s = 0$ as K_s does not vary so that $g = g_c + g_s = g_c$. Using Eq. (7) one obtains a formula valid up to zeroth order in U :

$$g = \frac{1}{2(4\pi v_F)^2} + O(U). \quad (9)$$

Some comments are in order. The expansion (7) is actually an expansion around $U = 0$ valid when $U \ll v_F$. When we move toward the BKT critical point one has $v_F \rightarrow 2$ and $g \rightarrow 1/(128\pi^2)$. This value is $3/16$ the number calculated directly at $U = 0$ in Sec. III A. We believe that this discrepancy is due to lattice corrections which are neglected in formula (8). Approaching the low density critical point $U = 0$, $n = 0$ Eq. (9) predicts that, in a narrow region $U \ll n$, the fidelity metric diverges as $g \sim n^{-2}$. This contrasts with the result $g \sim n^{-1}$ obtained at $U = 0$, as one would expect since U is a relevant perturbation. In fact, in the diluted regime, the low-energy effective theory is that of a spinful non-relativistic gas with delta interactions [18]. There one still has $n \sim |\mu - \mu_c|^{1/2}$ and dynamical exponent $\zeta = 2$. Thus if we take $\Delta_\mu = 1$, then using the conventional scaling analysis we would find $g \sim n^{-2}$, consistent with the bosonization result.

V. LUTTINGER PARAMETER AND BETHE-ANSATZ

The bosonization expression Eq. (7) is an expansion of $K_c(n, U)$ around $U = 0$ where K_c reaches its free Dirac value 1. In the whole stripe $U \geq 0$, $0 \leq n \leq 1$, $K_c(n, U)$ is a bounded function ranging between $1/2$ and 1 [26]. The maximal value $K_c = 1$ is obtained in the segment

$U = 0$. Instead the minimal value $K_c = 1/2$ is attained at the lines $n = 0$ and $n = 1$ and in the strong coupling limit, i.e. $K_c \rightarrow 1/2$ for $U \gg |t|$. This considerations show that, from Eq. (8), g can be infinite only at the points $U = 0$ and $n = 0$, or 1. However, from the results of the previous section one sees no divergence in the fidelity metric at the BKT point when this is approached from the $U \approx 0$ region. Let us now investigate what happens when we move to the BKT point from the $n \approx 1$ region.

To link Luttinger parameters to microscopic constants one generally uses [26]

$$\frac{\partial^2 e(n)}{\partial n^2} = \frac{\pi v_c}{2 K_c},$$

where $e(n)$ is the energy as a function of the filling. In Refs. [27, 28] a more efficient characterization of the Luttinger liquid parameter K_c in terms of Bethe Ansatz results has been found. K_c is related to the so called dressed charge function $\xi(k)$ through $K_c = \xi^2(Q)/2$. Using this equation, an expansion of K_c for filling close to 0 and 1 has been obtained in Refs. [28, 29]. At leading order, and calling $\delta = 1 - n$, they found

$$K_c = \frac{1}{2} + a(U)\delta + O(\delta^2), \quad (10)$$

where the function $a(U)$ is studied in the appendix and is approximately given by the following expansion, for $U/2\pi \ll 1$

$$a(U) \approx \frac{\ln(2)}{\sqrt{U}} e^{2\pi/U}.$$

Not surprisingly, this has the same form as the soliton length, $\xi(U)$. In fact $\xi(U) = \pi a(U)/2 \ln(2)$, for the regime of interest, $U/2\pi \ll 1$ [30].

The small doping expansion Eq. (10) is valid when $\delta \ll a^{-1}$ which defines a very narrow region

$$\delta \ll \frac{\sqrt{U}}{\ln 2} e^{-2\pi/U}, \quad (11)$$

marked with a hatched pattern in Fig. 1. Using again Eq. (8) we obtain for the metric tensor

$$g = \frac{1}{2} [a'(U)]^2 \delta^2 + O(\delta^3), \quad (12)$$

where now

$$[a'(U)]^2 \approx \frac{4\pi^2 \ln(2)^2}{U^5} e^{4\pi/U}.$$

Thus we see that in the region given by Eq. (11) and depending on the way we approach $U = 0$, $\delta = 0$, the fidelity metric g can diverge. For instance on the line given by $\gamma(t) = (U, \delta) = (t, \lambda\sqrt{t}e^{-2\pi/t})$, $\lambda \ll 0.45$, g diverges as

$$g(\gamma(t)) \sim t^{-4}.$$

Note however that from Eq. (12) g can tend to a constant if the BKT point is reached by sending δ to 0 faster than $\delta(U) \sim U^{5/2} e^{-2\pi/U}$.

The complementary region $\delta \gg a^{-1}$ is amenable to a perturbative renormalization group approach [31]. The Luttinger parameter takes the following form in the regime where $u \ln(Cn/\delta) \ll 1$ and $u \ll 1$:

$$K_c = 1 - \frac{u/2}{1 - u \ln(Cn/\delta)}.$$

Here $u = U/2\pi$ and C is a constant. Again using Eq. (8) we find $g \sim u^{-2} [1 - u \ln(Cn/\delta)]^{-4} \sim u^{-2} +$ smaller terms.

Similar considerations can be drawn around $n = 0$. In the low density limit we have an expansion similar to Eq. (10) with δ replaced by n and $a(U) = 4 \ln 2 / U$. The expansion now works in the dotted region of Fig. (1) which corresponds roughly to $n \ll U$. In this case the divergence around $n = 0$ is dictated by

$$(a')^2 = \frac{4(\ln 2)^2}{U^4}.$$

A path where a divergence can be observed is given by $\gamma(t) = (\lambda t, t)$, $\lambda \ll 1$, where one has $g(\gamma(t)) \sim t^{-2}$ as $t \rightarrow 0$. Again the divergence cannot be observed if the line $n = 0$ is approached too fast.

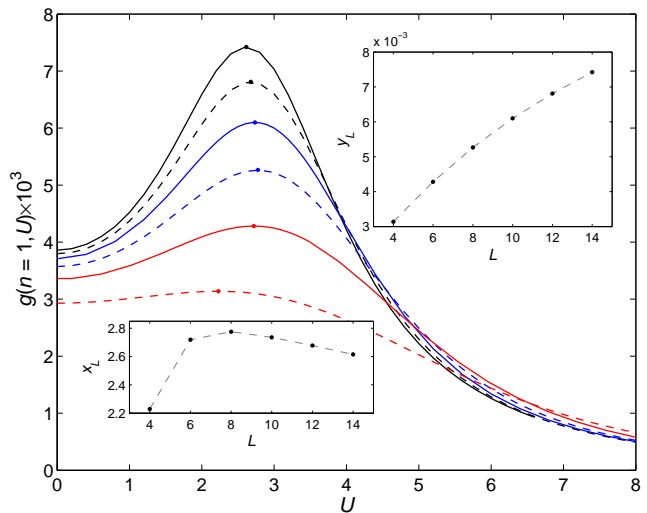


Figure 3: Scaling behavior of the intensive fidelity tensor at half filling. Dashed curves correspond, from bottom to top, to $L = 4, 8, 12$ (antiperiodic BC's), while solid curves, again from bottom to top, to $L = 6, 10, 14$ (periodic BC's). Note that at half filling $g(U)$ is symmetric around $U = 0$. In the insets the scaling of the position (x_L) and the height (y_L) of the maxima is shown.

VI. NUMERICAL ANALYSIS

As already reminded, on the line $n = 1$ the effective theory in the charge sector is the sine-Gordon model, with a charge gap for any $U > 0$. Correspondingly it is not possible to compute the fidelity metric using Eq. (8). We then resorted to numerical analysis on small system sizes. A similar analysis has appeared in Ref. [32], here we extend it to a larger data set $L = 14$ and draw some extra conclusions.

After calculating the ground state $\Psi_0(U)$ of Hamiltonian (1) with the Lanczos algorithm, the intensive fidelity metric g is obtained from the fidelity $F(U, U + \delta U) = |\langle \Psi_0(U) | \Psi_0(U + \delta U) \rangle|$ using

$$g_L = \frac{2}{L} \frac{1 - F(U, U + \delta U)}{\delta U^2}, \quad (13)$$

with $\delta U = 10^{-3}$. The above equation is a good approximation to the limit $\delta U \rightarrow 0$ as long as $\delta U \ll 1/\sqrt{Lg}$ which was confirmed to be the case in all simulations (see also Fig. (3)). In order to have as many data points as possible, we analyzed sizes of length $L = 4n+2$ with periodic boundary conditions (BC's), while for length $L = 4n$ antiperiodic boundary conditions were used. Choosing such boundary conditions, at half filling, assures that the ground state is non-degenerate even at $U = 0$ [38].

The numerical results are summarized in Fig. 3. The peaks observed at finite sizes might be a precursor of a divergence of the fidelity metric in the thermodynamic limit at the transition point $U = 0$, in the sense that $g(U \rightarrow 0^+) \rightarrow \infty$. To check this hypothesis the position (x_L) and the height (y_L) of the peaks are plotted in the inset as a function of the system size L . Concerning the peak height, fitting the three highest available data points with a power law $y_L = a_0 + a_1 L^\alpha$ gives $\alpha = 0.11$ whereas with a logarithmic correction of the form $y_L = b_0 + b_1 L^\beta \ln L$ we obtain $\beta = 0.06$. Both results indicate a super-extensive growth of the fidelity metric, and hence a divergence in the thermodynamic limit. However, the available sizes are too small to provide a conclusive answer.

VII. CONCLUSIONS

In this paper we analyzed, with a variety of analytical and numerical techniques, the one dimensional Hubbard model from the point of view of the recently proposed fidelity approach to quantum phase transitions. The main findings of this paper can be summarized as follows: i) An exact calculation, on the free gas line $U = 0$, shows that the fidelity metric g presents a cusp at half filling and a $1/n$ divergence at low density n respectively. ii) Using Bosonization techniques, we observe a divergence of the form $g \sim n^{-2}$ in the regime $U \ll n$ when $n \rightarrow 0$. iii) Resorting to Bethe Ansatz we extended the analysis to the regions of phase diagram where the Luttinger liquid parameter K_c approaches the strong coupling value

$1/2$ (roughly $n \gtrsim 0$ and $n \lesssim 1$). In these regions one observes divergences of g which depend on the way the critical point is approached. iv) Precisely at half filling the previous approaches do not apply and we resorted to numerical analysis. Our results, are not inconsistent with a divergence of the fidelity metric at $n = 1$ and $U \rightarrow 0^+$.

The presented analysis shows that the fidelity approach is able to characterize the rich phase diagram of a highly non trivial interacting many body system. In particular it provides valuable insights for the infinite order Mott transition occurring at half filling. The complete understanding of the behavior of the fidelity metric when $U \rightarrow 0^+$ at half filling, is an interesting issue which calls for future investigations.

The authors would like to thank Cristian Degli Esposti Boschi for a critical reading of the manuscript. The work of P.B. has been partially carried out in the framework of the PRIN project *Microscopic description of fermionic quantum devices*.

Appendix A:

Following Ref. [28] the coefficient a in Eq. (10) is given by

$$a(U) = \frac{4 \ln(2)}{U f(U)}$$

where

$$f(U) \equiv 1 - 2 \int_0^\infty \frac{J_0(x)}{1 + e^{Ux/2}} dx,$$

and J_0 is a Bessel function. Using the following results

$$\frac{1}{1 + e^{\alpha x}} = \sum_{n=0}^{\infty} (-1)^n e^{-(n+1)\alpha x}$$

$$\int_0^\infty J_0(x) e^{-\beta x} dx = \frac{1}{\sqrt{1 + \beta^2}}, \quad \alpha, \beta > 0,$$

we arrive at

$$f(U) = 1 + 2 \sum_{n=1}^{\infty} (-1)^n \frac{1}{\sqrt{1 + n^2 U^2/4}}.$$

Using the formalism of the Remnant Functions defined in Ref. [33] one realizes that $f(U)$ is related to $R_{1/2,0}^{(-)}(4U^{-2})$. With the help of the expansions in Ref. [33] we obtain the following expression

$$f(U) = \frac{8}{U} \sum_{n=0}^{\infty} K_0 \left(\frac{2\pi}{U} (2n+1) \right).$$

It is now easy to obtain the desired asymptotics, using the asymptotics of the Bessel function

$$K_0(1/x) = e^{-1/x} \sqrt{\frac{\pi x}{2}} \left(1 - \frac{1}{8}x + \frac{9}{128}x^2 + O(x^3) \right).$$

Collecting the results together, we obtain at leading order

$$a(U) = \frac{\ln(2)}{\sqrt{U}} e^{2\pi/U} (1 + O(U)).$$

-
- [1] P. Zanardi and N. Paunkovic, Phys. Rev. E **74**, 031123 (2006).
- [2] H. Q. Zhou and J. P. Barjaktarevic, arXiv:cond-mat/0701608.
- [3] P. Zanardi, M. Cozzini, and P. Giorda, J. Stat. Mech **2**, L02002 (2007).
- [4] M. Cozzini, P. Giorda, and P. Zanardi, Phys. Rev. B **75**, 014439 (2007).
- [5] M. Cozzini, R. Ionicioiu, and P. Zanardi, Phys. Rev. B **76**, 104420 (2007).
- [6] W. L. You, Y. W. Li, and S. J. Gu, Phys. Rev. E **76**, 022101 (2007).
- [7] S. J. Gu, H. M. Kwok, W. Q. Ning, and H. Q. Lin, arXiv:0706.2495.
- [8] H. Q. Zhou, arXiv:0704.2945.
- [9] P. Buonsante and A. Vezzani, Phys. Rev. Lett **98**, 110601 (2007).
- [10] A. Hamma, W. Zhang, S. Haas, and D. Lidar, arXiv:0705.0026.
- [11] H. Q. Zhou and B. L. J. H. Zhao, arXiv:0704.2940.
- [12] S. Chen, L. W. S. J. Gu, and Y. Wang, Phys. Rev. E **76**, 061108 (2007).
- [13] H. Q. Zhou, J. H. Zhao, H. L. Wang, and B. Li, arXiv:0711.465.
- [14] S. L. Zhu, Phys. Rev. Lett **96**, 077206 (2006).
- [15] M.-F. Yang, Phys. Rev. B **76**, 180403 (2007), note that recently the result of Yang for the fidelity metric has been corrected by a factor 1/2 [34].
- [16] P. Zanardi, P. Giorda, and M. Cozzini, Phys. Rev. Lett (2007).
- [17] L. Campos Venuti and P. Zanardi, Phys. Rev. Lett **99**, 095701 (2007).
- [18] F. H. L. Essler, H. Frahm, F. Göhmann, A. Klümper, and V. E. Korepin, *The One-Dimensional Hubbard Model* (Cambridge University Press, Cambridge, 2005).
- [19] J. Sólyom, Adv. Phys. **28**, 209 (1979).
- [20] J. Voit, Rep. Prog. Phys. **58**, 977 (1995), arXiv:cond-mat/9510014.
- [21] C. Itzykson and J.-M. Drouffe, *Statistical Field Theory* (Cambridge University Press, 1989).
- [22] S. Chen, L. Wang, Y. Hao, and Y. Wang, arXiv:0801.0020.
- [23] E. H. Lieb and F. Y. Wu, Phys. Rev. Lett **20**, 1445 (1968).
- [24] S. Sachdev, *Quantum Phase Transitions* (Cambridge University Press, 1999).
- [25] V. J. Emery, in *Highly Conducting One-Dimensional Solids* (Plenum, New York, 1979), p. 327.
- [26] H. J. Schulz, Phys. Rev. Lett **64**, 2831 (1990).
- [27] N. Kawakami and S.-K. Yang, Phys. Lett. A **148**, 359 (1990).
- [28] H. Frahm and V. E. Korepin, Phys. Rev. B **42**, 10553 (1990).
- [29] A. Schadschneider and J. Zittartz, Z. Phy. B **82**, 387 (1991).
- [30] C. A. Stafford and A. J. Millis, Phys. Rev. B **48**, 1409 (1993).
- [31] E. B. Kolomeisky and J. Straley, Rev. Mod. Phys **68**, 175 (1996).
- [32] W.-L. You, Y.-W. Li, and S.-J. Gu, Phys. Rev. E **76**, 022101 (2007).
- [33] M. E. Fisher and M. N. Barber, Arch. Rational Mech. Ann. **47**, 205 (1972).
- [34] J. O. Fjærestad, arXiv:0712.3439.
- [35] N. Laflorencie, S. Capponi, and E. S. Sorensen, Eur. Phys. J. B **24**, 77 (2001).
- [36] An almost standard route is that of adding an electric/magnetic field and to measure the corresponding stiffness which experiences a jump at the transition (see i.e. [35]).
- [37] The term BKT is justified in the sense that the underlying effective theory is the sine-Gordon model (see later). In the condensed matter literature the term Mott transition is more commonly used.
- [38] Note also that both these classes of fermionic systems with different boundary conditions, can be mapped onto an interacting systems of hard-core bosons with periodic boundary conditions. This clarifies further why it is possible to compare data obtained with different boundary conditions.